Common Phase Diagram for Antiferromagnetism in $La_{2-x}Sr_xCuO_4$ and $Y_{1-x}Ca_xBa_2Cu_3O_6$ as Seen by Muon Spin Rotation

Ch. Niedermayer,[1] C. Bernhard,[2] T. Blasius,[1] A. Golnik,[3] A. Moodenbaugh,[4] and J. I. Budnick[5]
[1]*Fakultät für Physik, Universität Konstanz, D-78434 Konstanz, Germany*
[2]*Max-Planck-Institut für Festkörperforschung, D-70569 Stuttgart, Germany*
[3]*Institute of Experimental Physics, Warsaw University, PL-00-681 Warsaw, Poland*
[4]*Department of Applied Science, Brookhaven National Laboratory, Upton, New York 11977*
[5]*Department of Physics and Institute of Materials Science, University of Connecticut, Storrs, Connecticut 06269*
(Received 19 September 1997)

By zero field muon spin rotation we studied the antiferromagnetic correlations in the single layer system $La_{2-x}Sr_xCuO_4$ and the bilayer system $Y_{1-x}Ca_xBa_2Cu_3O_6$. We observe a common phase diagram as a function of hole doping per plane with two distinct transitions in the magnetic ground state. The first transition marks the border between the 3D antiferromagnetic state and a disordered state with short ranged correlations. The second transition marks a distinct change in the magnetic correlations at the onset of superconductivity. [S0031-9007(98)05990-0]

PACS numbers: 74.25.Ha, 74.62.Dh, 76.75.+i

A characteristic feature of the cuprate high-T_c superconductors is the strong dependence of their magnetic and superconducting (SC) properties on the number of holes doped into the CuO_2 planes. The undoped compounds La_2CuO_4 and $YBa_2Cu_3O_6$ are insulators and exhibit long range 3D antiferromagnetic (AF) order, which is rapidly destroyed as holes are doped into the CuO_2 planes. Superconductivity occurs beyond a critical hole content of $p_{sh} \approx 0.05-0.06$, where p_{sh} is the fraction of doped holes per Cu atom in the CuO_2 sheet. The critical temperature $T_c(p_{sh})$ follows a universal, approximately parabolic p_{sh} dependence, which appears to be common to the high-T_c cuprates, and all that varies is the optimal value $T_{c,\max}$ [1,2]. In $La_{2-x}Sr_xCuO_4$ (La,Sr-214) a short range ordered AF state is known to persist at intermediate doping for $0.02 < p_{sh} < 0.05$. Previous muon spin rotation (μSR) studies on La,Sr-214 have indicated that this short range AF correlated state even coexists with SC in the strongly underdoped regime for $0.05 < p_{sh} < 0.1$ [3]. For the $YBa_2Cu_3O_{7-\delta}$ (Y-123) system, the regime of low doping is not readily accessible since the hole transfer from the CuO chains to the CuO_2 planes is rather complex and depends critically on oxygen ordering and content. In this paper, we present the results of an extensive μSR reinvestigation of the doping dependence of the AF correlation in polycrystalline La,Sr-214 samples. In addition, we studied the bilayer compound $Y_{1-x}Ca_xBa_2Cu_3O_6$ (Y,Ca-123) for which, because of the unoccupied chains, p_{sh} can be adjusted in a controlled way through the substitution of Y^{3+} by Ca^{2+}. We obtain a common magnetic phase diagram as a function of *one parameter*, p_{sh}, which suggests that we observe the intrinsic property of the electronic ground state of the CuO_2 planes.

A series of powder La,Sr-214 samples was prepared using conventional ceramic techniques. The preparation of Y,Ca-123 samples has been described previously [2]. From neutron refinement, the occupancy of Ca on the Y site was found to be close to 100% up to $x = 0.15$ [2] but somewhat reduced for higher Ca content, i.e., $x_{\rm eff} = 0.18$ in the case of $x = 0.2$. The substitution of Y^{3+} by Ca^{2+} produces holes in the CuO_2 planes giving $p_{sh} = x_{\rm eff}/2$. This is indicated by the variation of T_c with Ca content (for fixed oxygen content) and has been confirmed by optical studies [4], by measurements of the thermoelectric power and by bond-valence sum calculations [2].

The zero field muon spin rotation (ZF-μSR) technique [5] is especially suited for the study of weak and short range magnetic correlations, since the positive muon is an extremely sensitive local probe able to detect internal magnetic fields as small as 0.1 mT and covering a time window from 10^{-6} s to about 10^{-9} s. The μSR experiments were performed at the Paul-Scherrer-Institut in Villigen, Switzerland and at TRIUMF in Vancouver, Canada. Representative ZF-μSR time spectra are shown in Fig. 1. At low temperature and for $p_{sh} \leq 0.08$, the time evolution of the muon spin polarization is well described by the ansatz:

$$G_z(t) = \frac{2}{3}\cos(\gamma_\mu B_\mu t + \Phi)\exp\left(-\frac{1}{2}(\gamma_\mu \Delta B_\mu t)^2\right) + \frac{1}{3}\exp(-\lambda t),$$

where $\gamma_\mu = 851.4$ MHz/T is the gyromagnetic ratio of the muon, B_μ the average internal magnetic field at the muon site, and ΔB its rms deviation. The two terms arise from the random orientation of the local magnetic field in a polycrystalline sample, which on average points parallel (perpendicular) to the muon spin direction with probability $\frac{1}{3}$ ($\frac{2}{3}$) [5]. In analogy to NMR the dynamic spin lattice relaxation rate $\lambda = 1/T_1$ is given by

$$\frac{1}{T_1} = \gamma_\mu^2 \langle B_t^2 \rangle \frac{\tau_c}{1 + (\omega_\mu \tau_c)^2}.$$

A slowing down of magnetic fluctuations typically causes a maximum of $1/T_1$ at $\omega_\mu \tau_c \approx 1$, where ω_μ is the

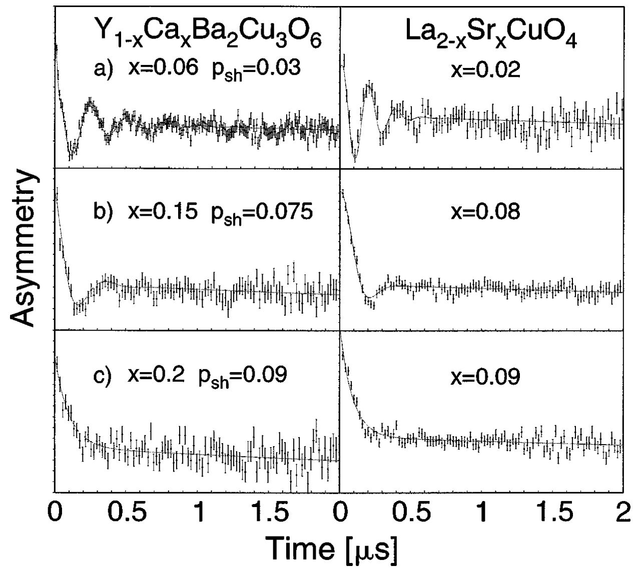

FIG. 1. ZF-μSR spectra obtained at low temperatures ($T < 1$ K) for various degrees of hole doping in $Y_{1-x}Ca_xBa_2Cu_3O_{6.02(1)}$ and $La_{2-x}Sr_xCuO_4$. Dotted curves are the fit to the data using Eq. (1).

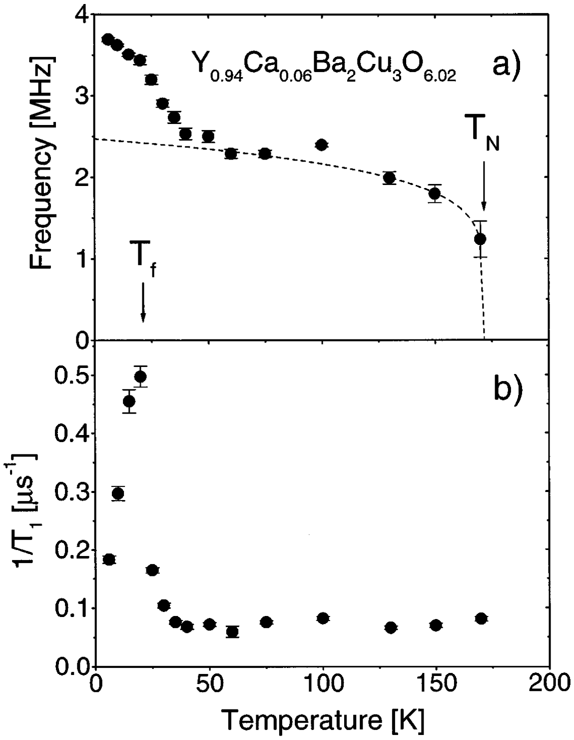

FIG. 2. ZF-μSR results on $Y_{0.94}Ca_{0.06}Ba_2Cu_3O_{6.02(1)}$ plotted as a function of temperature. (a) The muon spin precession frequency and (b) the longitudinal relaxation rate $1/T_1$. The dotted line in (a) represents a fit of the data with a power law $(1 - T/T_N)^\beta$ with $\beta = 0.2$.

μ^+ Zeeman frequency, $\langle B_t^2 \rangle$ is the mean of the square of the fluctuating transverse field components, and τ_c is their average correlation time. A precessing $\frac{2}{3}$ component indicates static magnetic order on the time scale of the μSR technique ($\tau_c < 10^{-6}$ s). For $p_{\mathrm{sh}} > 0.08$, no oscillations were observed and the $\frac{2}{3}$ part of $G_z(t)$ was better represented by an exponential relaxation $\exp(-\Lambda t)$ [see Fig. 1(c)], which may indicate either a very strongly disordered static field distribution or rapid fluctuations.

The phase diagram as a function of hole doping exhibits three distinct magnetic regimes. In regime I of the undoped and lightly doped systems, the Cu^{2+} spins and those of the holes order independently. As an example, we discuss the data on $Y_{0.94}Ca_{0.06}Ba_2Cu_3O_{6.02}$ which are displayed in Fig. 2. Well below the 3D Néel temperature of $T_N \sim 170$ K a second magnetic transition occurs at a temperature $T_f \sim 25$ K. This is evident from the peak in the longitudinal relaxation rate $1/T_1$ and the upturn of the muon spin precession frequency. A corresponding transition within the AF state has been reported recently from La-NQR [6] and μSR studies [7] on La,Sr-214, where $T_f = (815\text{ K}) \cdot p_{\mathrm{sh}}$ has been obtained for $p_{\mathrm{sh}} < 0.02$. This transition was ascribed to a freezing of the spins of the doped holes into a spin-glass state which is superimposed on the preexisting 3D AF long range order of the Cu^{2+} spins. Interestingly, we find that the spin freezing temperature T_f exhibits the same linear dependence on the planar hole content for Y,Ca-123 and La,Sr-214 [see Fig. 3(a)]. According to the model of Gooding *et al.* [8], in which $k_B T_f \approx J_{\mathrm{eff}} p_{\mathrm{sh}}$, this implies that the effective in-plane exchange coupling constant J_{eff} is identical for both systems and the freezing of the spin degrees of freedom is a property of the hole dynamics *within a single plane*. The Néel state, however, persists to higher hole content in Y,Ca-123 ($0 \le p_{\mathrm{sh}} \le 0.035$) as compared to La,Sr-214 ($p_{\mathrm{sh}} \le 0.02$). This suggests that the bilayer coupling makes the 3D AF state more robust to the presence of doped holes. A similar result was reported from a ^{89}Y NMR study of T_N in Y,Ca-123 [9].

Only a single magnetic transition into a short range AF correlated spin-glass-like state [10] is observed in regime II for $p_{\mathrm{sh}} > 0.02$ in La,Sr-214 [11] and $p_{\mathrm{sh}} > 0.035$ in Y,Ca-123. This transition is characterized by a slowing down of the AF fluctuations towards a glass transition which is defined by the maximum in $1/T_1$ (corresponding to a correlation time of the spin fluctuations of about 10^{-7} s). T_g is significantly higher due to bilayer interactions in Y,Ca-123 than in La,Sr-214. It is remarkable that the average internal field at the muon site is only modestly reduced in regime II (as compared to regime I) while the transition temperature is lowered by about 1 order of magnitude. This is illustrated in Fig. 3(b), where we display the zero temperature limit of the internal field at the muon site normalized to its value at zero doping, $B_\mu(T = 0, p_{\mathrm{sh}})/B_\mu(T = 0, p_{\mathrm{sh}} = 0)$. The width of the field distribution ΔB, which is a measure of the degree of disorder of the magnetic state, increases in this regime with hole doping, as can be seen in Fig. 3(c). The modest reduction of the average internal field in regime II and the strong increase of ΔB with hole doping can be

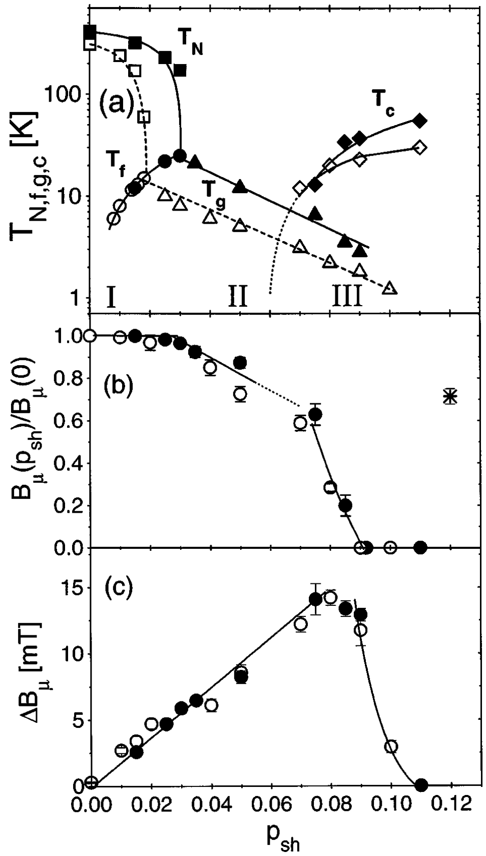

FIG. 3. Magnetic phase diagrams as a function of the hole concentration per CuO_2 sheet for $La_{2-x}Sr_xCuO_4$ (open symbols) and $Y_{1-x}Ca_xBa_2Cu_3O_{6.02}$ (solid symbols). (a) In regime I, two transitions are observed. The Néel temperatures T_N (squares), at which the Cu^{2+} spins order into a 3D AF state and a freezing transition of the spins of the doped holes at $T_f = (815\text{ K})p_{\text{sh}}$ (circles, including data from Ref. [7]). T_g indicates a transition into a spin-glass-like state (up triangles, regime II) with strong magnetic correlations which coexist with superconductivity in regime III. Diamonds represent the superconducting transition temperatures. (b) Doping dependence of the normalized average internal magnetic field at the muon site. The star at $p_{\text{sh}} = 0.12$ represents the data for $La_{1.58}Nd_{0.3}Sr_{0.12}CuO_4$. (c) The rms deviation ΔB. Data in (b) and (c) are for $T < 1$ K.

understood in terms of a phase separated electronic state, where the holes segregate into metallic domains leaving mesoscopic hole poor regions with AF strongly correlated Cu^{2+} spins. The AF order then is limited mainly by finite size effects [6,12,13], where the size L of the AF domains is determined by the hole content, $L(p_{\text{sh}}) \sim (1/p_{\text{sh}})^{1/2}$. The spin-glass temperature is then expected to vary as $T_g \sim L^2(p_{\text{sh}}) \sim 1/p_{\text{sh}}$ [14], in qualitative agreement with experiment. Unlike conventional spin glasses, the magnetic moments undergoing the glass transition arise from extended AF correlated domains. Accordingly, this state has been termed a "cluster spin glass."

The spin glass regime extends far into the SC state (regime III). For strongly underdoped SC samples with $0.06 < p_{\text{sh}} < 0.10$, we still observe a freezing of the spin degrees of freedom. Except for the somewhat smaller ordering temperature, the signature of the transition is the same as for the non-SC samples in regime II. From the amplitude of the rapidly damped muon spin polarization [see Figs. 1(b) and 1(c)], we can obtain information about the volume fraction of the magnetically correlated regions. We find that all of the muons stopped inside the sample experience a nonzero local magnetic field, which implies that the magnetic order persists throughout the entire volume of the sample. The magnetic ground state may still be inhomogeneous but the size of the nonmagnetic hole-rich regions must be smaller than the typical length scale (about 20 Å) of the μSR experiment. By decoupling experiments in a longitudinal field we have confirmed the static nature of the magnetic ground state [15]. From transverse field measurements we find that the flux line lattice which is formed below $T_c > T_g$ extends throughout the entire volume of the sample [16]. Note, that these results are markedly different from the μSR results that have been obtained on the "superoxide" $La_2CuO_{4.13}$, where long range oxygen diffusion leads to macroscopic phase separation with an average domain size of about 3000 Å [17]. In this compound, finite-size effects are negligible and the hole-poor phase (40% of the volume fraction) displays a temperature dependence and absolute values of the internal fields identical to those in stoichiometric La_2CuO_4. Simultaneously, a flux line lattice forms only within the hole-rich regions which accounts for the remaining 60% of the volume [18]. As described above, our present μSR results are fundamentally different and indicate a microscopic coexistence of the AF and SC order parameter. We want to stress that identical magnetic behavior is observed for both the single layer system La,Sr-214 and the bilayer compound Y,Ca-123.

The consistency of our results suggests that the coexistence of SC and AF order is an intrinsic property of the CuO_2 planes and not an artifact of chemical or structural impurities. Our data show that the strength of the AF correlation is determined solely by the hole content of the CuO_2 planes and does not depend on the concentration of dopant atoms. For a given hole content the number of dopant atoms (Ca^{2+} or Sr^{2+}) is twice the number in Y,Ca-123 compared to La,Sr-214.

In contrast to T_g which evolves rather smoothly, the internal magnetic field at the muon site exhibits a strong change for $p_{\text{sh}} \approx 0.06 - 0.08$ as one enters the SC regime. The change in slope is rather significant and indicates a distinct change in the ground state properties of the CuO_2 planes. From the μSR experiment alone, we cannot decide whether it is the competition between the AF and the SC order parameter or an underlying change of the electronic properties of the CuO_2 planes which causes the suppression of the internal field. Further experiments will be required in order to clarify if the SC order parameter is affected by the static AF correlation.

Notably, the AF correlation is fully restored at $p_{\text{sh}} \approx \frac{1}{8}$. A depression of T_c at this hole concentration at first

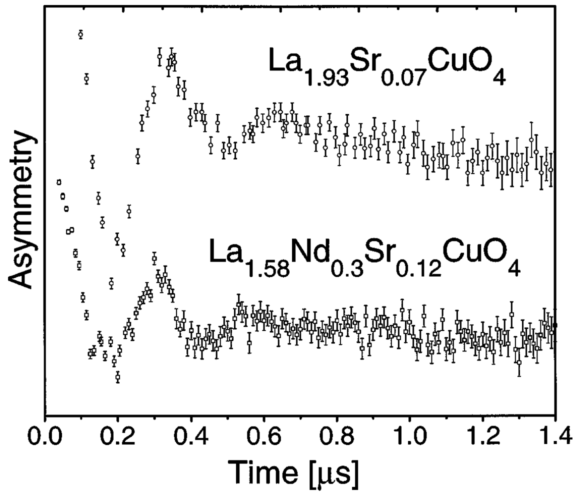

FIG. 4. ZF-μSR spectra of $La_{1.93}Sr_{0.07}CuO_4$ and $La_{1.58}Nd_{0.3}Sr_{0.12}CuO_4$ for $T = 100$ mK and $T = 10$ K, respectively. The latter temperature was chosen to avoid the extra complications associated with the effects of the slowing down of the Nd moments below this temperature.

appeared to be uniquely present in $La_{2-x}Ba_xCuO_4$ [19], but recent studies on $La_{2-x}Sr_xCuO_4$ [20] have shown the presence of a shallow cusp at the same doping level, and this behavior may also be related to the 60 K plateau in Y-123 [21]. Detailed μSR studies by Luke *et al.* and Kumagai *et al.* [22] show that at this doping level static magnetic order is restored at temperatures below 35 K. Tranquada *et al.* [23] showed that the static order in $La_{1.6-0.125}Nd_{0.4}Ba_{0.125}CuO_4$ comprised a spatial separation of the spin and charge into AF stripes three lattice spacings wide (hole poor) separated by antiphase domain boundaries of one lattice dimension where the doped holes reside on every second site. If we consider a picture in which a stripe phase were to be established through connectivity of the hole doped regions already existing in regime II, the averaged internal magnetic field is expected to be 75% of the value of the undoped compound. Interestingly, this value is observed for both the SC compound $La_{1.93}Sr_{0.07}CuO_4$ and the non-SC static stripe phase compound $La_{1.58}Nd_{0.3}Sr_{0.12}CuO_4$. Moreover, as displayed in Fig. 4, the measured time evolution of the muon spin asymmetry is almost identical for both compounds, suggesting the presence of similar local magnetic order.

In summary, we have studied the magnetic phase diagram for the single layer system $La_{2-x}Sr_xCuO_4$ and the bilayer compound $Y_{1-x}Ca_xBa_2Cu_3O_6$. We observe a common phase diagram which is characterized by two distinct transitions of the magnetic ground state. In the 3D AF regime we observe a freezing of the spin degrees of freedom of the doped holes at a temperature T_f, which increases linearly with the number of doped holes in both systems, suggesting that the hole dynamics in a single plane is responsible for the observed behavior. Because of plane to plane correlations, this regime extends to higher hole concentrations in the bilayer system. For higher doping levels (regime II), we observe a single magnetic transition into a spin-glass-like state with T_g(Y,Ca-123) $> T_g$(La,Sr-214) and extending well into the superconducting regime III. The evolution of the internal magnetic field with doping is understood on the basis of a microscopic phase segregation of the doped holes into hole-rich and hole-poor regions. We observe a microscopic coexistence of superconductivity and frozen antiferromagnetic correlations at low temperatures for underdoped samples. The strength of the AF correlations is determined by the *planar hole content* and does not depend on the concentration of dopant atoms. The rapid reduction of the internal magnetic field for the SC samples may suggest some competition between the AF and the SC order parameters, where the sublattice magnetization is reduced with the onset of superconductivity.

We would like to thank C. Baines, D. Herlach, and S. Kreitzman for technical support during the experiments. We are grateful to E. J. Ansaldo, C. Bucci, G. Guidi, D. R. Noakes, R. DeRenzi, C. E. Stronach, and X. Wan, who collaborated on part of the experiments. The authors acknowledge J. L. Tallon and V. J. Emery for fruitful discussions. The financial support of the German BMBF is gratefully acknowledged.

[1] M. R. Presland *et al.*, Physica (Amsterdam) **176C**, 95 (1991).
[2] J. L. Tallon *et al.*, Phys. Rev. B **51**, 12 911 (1995).
[3] A. Weidinger *et al.*, Phys. Rev. Lett. **62**, 102 (1989); H. Kitazawa *et al.*, Solid State Commun. **67**, 1191 (1988); E. Torikai *et al.*, Hyperfine Interact. **63**, 271 (1990).
[4] K. Widder *et al.*, Physica (Amsterdam) **267C**, 254 (1996).
[5] A. Schenck, *Muon Spin Rotation: Principles and Applications in Solid State Physics* (Adam Hilger, Bristol, 1986).
[6] F. C. Chou *et al.*, Phys. Rev. Lett. **71**, 2323 (1993).
[7] F. Borsa *et al.*, Phys. Rev. B **52**, 7334 (1995).
[8] R. J. Gooding *et al.*, Phys. Rev. B **49**, 6067 (1994).
[9] H. Casalta *et al.*, Physica (Amsterdam) **204C**, 331 (1993).
[10] F. C. Chou *et al.*, Phys. Rev. Lett. **75**, 2204 (1995).
[11] J. I. Budnick *et al.*, Europhys. Lett. **5**, 65 (1988).
[12] V. J. Emery and S. A. Kivelson, Physica (Amsterdam) **209C**, 597 (1993).
[13] D. C. Johnston *et al.*, Physica (Amsterdam) **235C–240C**, 257 (1994).
[14] J. H. Cho *et al.*, Phys. Rev. B **46**, 3179 (1992).
[15] Ch. Niedermayer *et al.* (to be published).
[16] C. Bernhard *et al.*, Phys. Rev. B **52**, 10 488 (1995).
[17] J. D. Jorgensen *et al.*, Phys. Rev. B **38**, 11 337 (1988).
[18] E. J. Ansaldo *et al.*, Phys. Rev. B **40**, 2555 (1989).
[19] A. R. Moodenbaugh *et al.*, Phys. Rev. B **38**, 4596 (1988).
[20] P. G. Radaelli *et al.*, Phys. Rev. B **49**, 4163 (1994).
[21] J. L. Tallon *et al.*, Physica (Amsterdam) **282C–287C**, 236 (1997).
[22] G. M. Luke *et al.*, Physica (Amsterdam) **185C–189C**, 1175 (1991); K. Kumagai *et al.*, Physica (Amsterdam) **185C–189C**, 913 (1991).
[23] J. M. Tranquada *et al.*, Phys. Rev. Lett. **78**, 338 (1997).